Segmentation of Branching Vascular Structures using Adaptive Subdivision Surface Fitting

Pieter H. Kitslaar[1,2], Ronald van 't Klooster[1], Marius Staring[1], Boudewijn P.F. Lelieveldt[1] and Rob J. van der Geest[1]

[1]Division of Image Processing, Department of Radiology, Leiden University Medical Center, Leiden, The Netherlands;
[2]Medis medical imaging systems b.v., Leiden, The Netherlands;

ABSTRACT

This paper describes a novel method for segmentation and modeling of branching vessel structures in medical images using adaptive subdivision surfaces fitting. The method starts with a rough initial skeleton model of the vessel structure. A coarse triangular control mesh consisting of hexagonal rings and dedicated bifurcation elements is constructed from this skeleton. Special attention is paid to ensure a topological sound control mesh is created around the bifurcation areas. Then, a smooth tubular surface is obtained from this coarse mesh using a standard subdivision scheme. This subdivision surface is iteratively fitted to the image. During the fitting, the target update locations of the subdivision surface are obtained using a scanline search along the surface normals, finding the maximum gradient magnitude (of the imaging data). In addition to this surface fitting framework, we propose an adaptive mesh refinement scheme. In this step the coarse control mesh topology is updated based on the current segmentation result, enabling adaptation to varying vessel lumen diameters. This enhances the robustness and flexibility of the method and reduces the amount of prior knowledge needed to create the initial skeletal model. The method was applied to publicly available CTA data from the Carotid Bifurcation Algorithm Evaluation Framework[1] resulting in an average dice index of 89.2% with the ground truth. Application of the method to the complex vascular structure of a coronary artery tree in CTA and to MRI images were performed to show the versatility and flexibility of the proposed framework.

Keywords: subdivision, vessel, segmentation, modeling

1. DESCRIPTION OF PURPOSE

Vessel segmentation remains an active topic in the medical image analysis and clinical community. Robust and accurate vessel segmentation is needed for efficient navigation and visualization of often complex vascular systems. Furthermore, quantitative parameters obtained from vascular images (e.g. degree of stenosis) are increasingly being used for diagnosis and medical treatment planning. Also, due to the increase in computational power the use of computational fluid dynamics (CFD) to simulate blood flow in vascular systems receives growing interest. For these simulations accurate and smooth vessel boundaries are required to define a good computational domain and achieve correct results.

Numerous vessel segmentation approaches have already been published.[2] One of the best known methods for segmentation of vascular (branching) structures are level-sets.[3] However, these often require high computational costs and suffer from leakage which includes unwanted structures (and irregularities) in the final segmentation. Also, optimal surface segmentation[4] has shown to produce accurate and robust results. However, it requires the mapping (or unfolding) of the vascular structure to a rectangular grid which is non-trivial near bifurcations.

We propose a novel vascular segmentation method in which a subdivision surface is adaptively fitted to vascular image data. Subdivision surfaces provide a smooth boundary surface which is controlled by a coarse control mesh with local support. We present an elegant way to construct a coarse control mesh for branching vascular systems based on the use of dedicated bifurcation templates. This system allows to easily describe arbitrary vascular topologies consisting of numerous bifurcations. We also present an adaptive refinement scheme where the structure of the coarse control mesh can be iteratively updated to better reflect the target vascular system. The proposed framework is elegant and has the advantage of being fast and flexible.
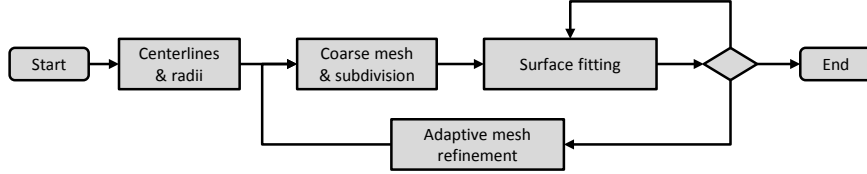
Figure 1: Subdivision segmentation framework overview.

2. METHODS

Figure 1 shows an overview of the segmentation framework in which a subdivision surface is iteratively fitted to the image data. The initial input to the framework is a set of centerlines with associated radii. From these centerlines an initial coarse mesh model is constructed and the corresponding subdivision surface is calculated. Next, one or more iteration steps are performed where the coarse mesh model is updated based on the image forces acting on the subdivision surface. After these fitting steps an adaptive mesh refinement can be performed, which updates the topology of the coarse mesh model to best reflect the current segmentation result. After this a new round of fitting iterations can be initiated.

The various parts of the segmentation scheme are discussed below. First, more information about subdivision surfaces and how they can be iteratively fitted to image data is given. Next, the details about the construction of the coarse control mesh from a set of centerlines are presented. Finally, the adaptive mesh refinement part of the segmentation scheme is described.

2.1 Subdivision Surfaces

In the computer graphics industry, subdivision schemes are extensively used to create a smooth surface based on a coarse mesh (Fig 2a). Subdivision surfaces have been occasionally used in image segmentation[5] and registration.[6]

A subdivision surface is constructed from a coarse control mesh by adding additional vertices to the original mesh and updating the positions of the existing vertices. The position of these subdivision surface points $\mathbf{p}_j$, is a weighted average of the control vertices $\mathbf{q}_i$ in a local neighborhood. The exact weights and neighborhoods are defined by the chosen subdivision scheme. In this work the Loop subdivision scheme was used.[7] Figure 2b depicts the weights and neighborhood for the Loop subdivision scheme. During the subdivision procedure the control vertices (indexed by i) and the associated weights used to define the surface points (indexed by j) are stored in the weight matrix $w_{i,j}$. Once this matrix is computed it can be used to efficiently compute the updated position of the surface points due to changes of the control vertices. This matrix only needs to be computed once or whenever the topology of the coarse control mesh changes as part of the adaptive mesh refinement (as discussed in Section 2.3). Also, the matrix $w_{i,j}$ is very sparse since the relation between surface and control points is only defined within a local neighborhood and can be efficiently stored in computer memory.

2.1.1 Fitting a Subdivision Surface to Image Data.

During each iteration (indexed by t) the subdivision surface is deformed by updating the position of the control vertices. First, a force vector $\mathbf{f}_j^t$, based on local image information, is calculated for each surface point position $\mathbf{p}_j^t$. From these forces the new position of the control vertices is computed as:

$$\mathbf{q}_i^{t+1} = \mathbf{q}_i^t + \alpha \frac{\sum_j w_{i,j} \mathbf{f}_j^t}{\sum_j w_{i,j}}, \tag{1}$$

where α is a global force factor $[0,1]$ which can be used to regularize the fitting.

After all new positions of the control vertices are calculated the new position of the subdivision surface vertices is updated as:

$$\mathbf{p}_j^{t+1} = \sum_i w_{i,j} \mathbf{q}_i^{t+1}, \tag{2}$$
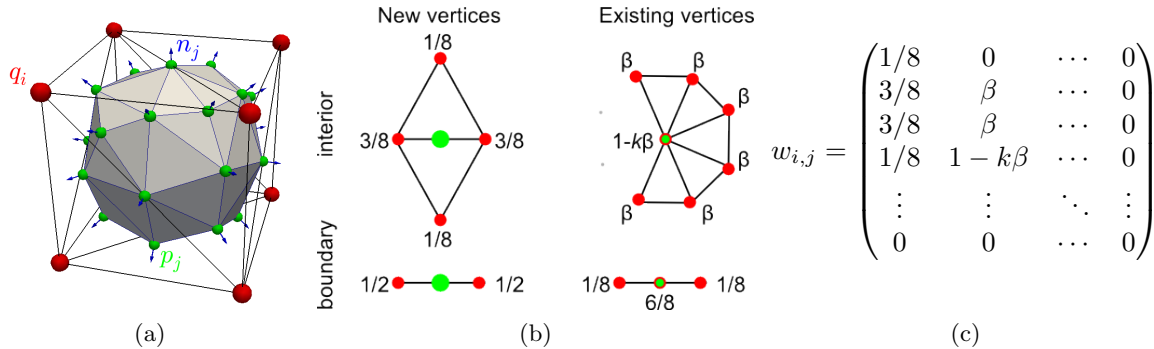
Figure 2: (a) Example of a control mesh and the corresponding subdivision surface. The nodes $\mathbf{q}_i$ (red) are the course control vertices, and the nodes $\mathbf{p}_j$ (green) the surface points obtained from the subdivision algorithm. The vectors $\mathbf{n}_j$ (blue) indicate the surface normals. (b) The weights and vertex neighborhood used for the Loop subdivision scheme.[7] In the scheme $\beta = 1/k(5/8 - (3/8 + 1/4\cos(2\pi/k)^2))$, where k is the number of connected edges to the target vertex. (c) Example of the structure of the weight matrix $w_{i,j}$.

2.1.2 Image forces

The force $\mathbf{f}_j$ indicates how $\mathbf{p}_j$ should move to obtain the desired segmentation result. In principle the method used to compute these forces is independent from the design of the presented iterative subdivision fitting framework. Usually for segmentation purposes the forces will be computed based on image data, but they could also be based on other information like implicit functions, internal model forces (based on the current state of the geometry) or manually indicated annotations.

In this work we choose $\mathbf{f}_j$ to act along the surface normal $\mathbf{n}_j$ through $\mathbf{p}_j$. We find the point $\mathbf{x}_j$ along the normal with maximum gradient magnitude, i.e. we solve

$$\mathbf{x}_j = \arg\max_{\mathbf{x}_k \in \mathcal{S}_j} \|\nabla I(\mathbf{x}_k)\|, \tag{3}$$

where the scanline $\mathcal{S}_j$ contains the set of points along the normal within a distance l^+ from $\mathbf{p}_j$ in the positive normal direction (outside of the surface) and a distance l^- in the negative normal direction (inside of the surface). The image force is then defined as $\mathbf{f}_j = \mathbf{x}_j - \mathbf{p}_j$. The ratio between the chosen values for l^+ and l^- can be used to prefer an outward or inward search for image borders from the current surface position.

Figure 3 shows examples of scanlines and their computed forces on the surface in a CTA dataset from the cls2009[1] challenge.

2.2 Coarse Mesh Model Construction.

A large part of the elegance of the proposed segmentation framework lies in the construction of the coarse mesh model for the bifurcating vascular system from the skeletal centerlines with associated radii.

For the initial construction of the coarse mesh model we assume that an appropriate set of skeleton centerlines with associated radii information is available. These could be obtained using automated vessel tracking techniques or from a number of manually annotated positions in the target image. Due to the adaptive refinement step (discussed later), the radii information for the initial centerlines does not have to be accurate and could even be assumed to be constant for all the centerlines during the initial model building.

To obtain a coarse mesh model from the input skeleton centerlines we follow a number of steps. The idea for the use of hexagonal rings and the details of the bifurcation connection scheme described below are to a large extent based on work by MacMurchy[8] which contains a description of building surface representations for the modeling of plants. We adapted this work for the modeling of vascular structures.
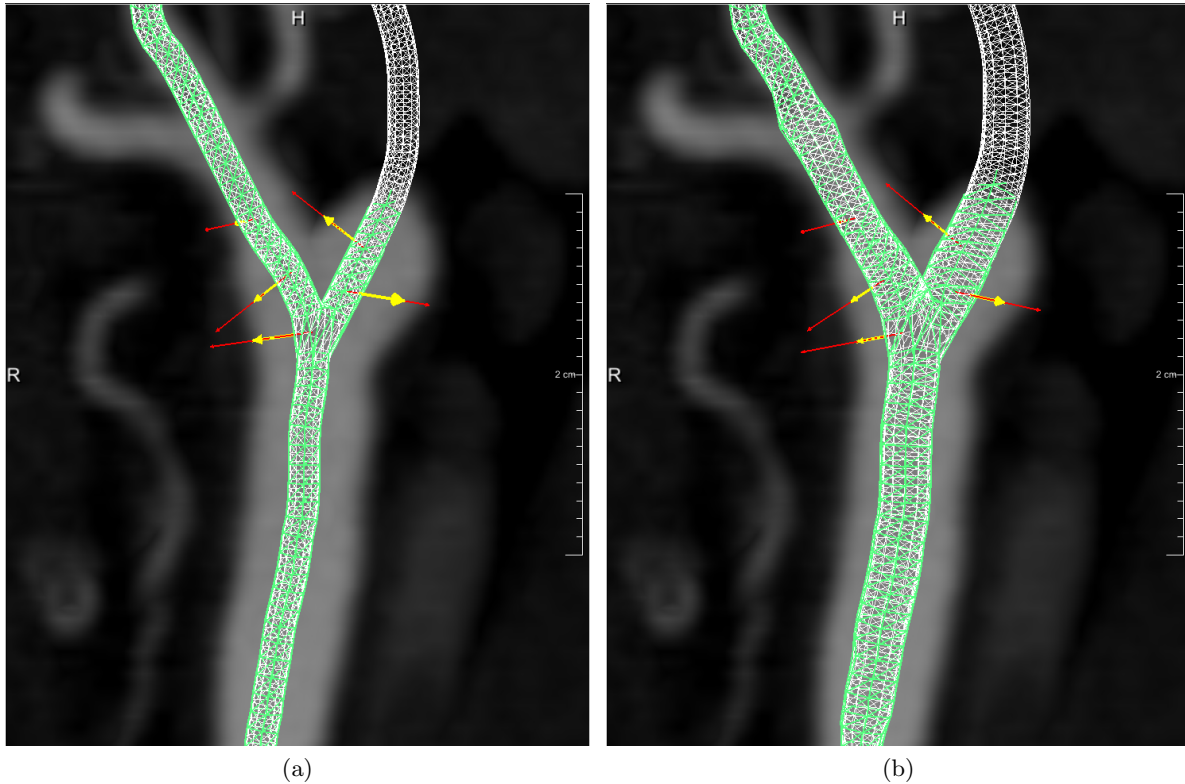
Figure 3: Example of a selected number of scanlines (red) and force vectors (yellow with arrow head) computed on the subdivision surface (white) obtained from the coarse control mesh (green) during the first iteration (a) and the next iteration (b). The image data shows a thick slab MIP projection of CTA data from Challenge000 patient of cls2009.[1]

2.2.1 Hierarchical tree

At the start, the set of input centerlines are analyzed to generate a hierarchical tree structure where each branch has an associated parent branch and two (or more) associated child branches. Furthermore, at bifurcations the overlapping regions of the different child and parent branches are defined. These bifurcation regions (whose sizes are proportional to the radii of the associated branches) are used to define non-overlapping centerlines for the branches in the tree. Also, these open regions provide space for the placement of dedicated bifurcation geometry (see Section 2.2.3). The branch hierarchy analysis and calculation of the bifurcation region is based on the method described by Antiga et al.[9] which is available as part of the Vascular Modeling ToolKit (`http://www.vmtk.org`).

2.2.2 Branches

The basic structural elements of the coarse mesh for the individual branches (e.g. between two bifurcations or start/end points) in the vascular tree are hexagonal rings which are placed along the centerlines and connected with each other. The orientation of the hexagonal ring is defined by the local tangent direction of the centerline (see Figure 4a). The radii of the hexagonal rings depend on the radii information available at the associated centerline positions. Furthermore, the distance between the rings on the centerlines (and therefore the number of rings) also depends on the radii information. A smaller ring distance is used when the radius decreases (Fig. 4b). This ring distance adaptation is used so the final surface model has more freedom to follow the (local) changes in diameter in the vessel (for example at a stenosis).

2.2.3 Bifurcations

At bifurcations, the three (or more for higher order junctions) rings from the main branch and the side branches need to be connected to form a closed surface. Obtaining a simple description for constructing these bifurcation

(a)   (b)
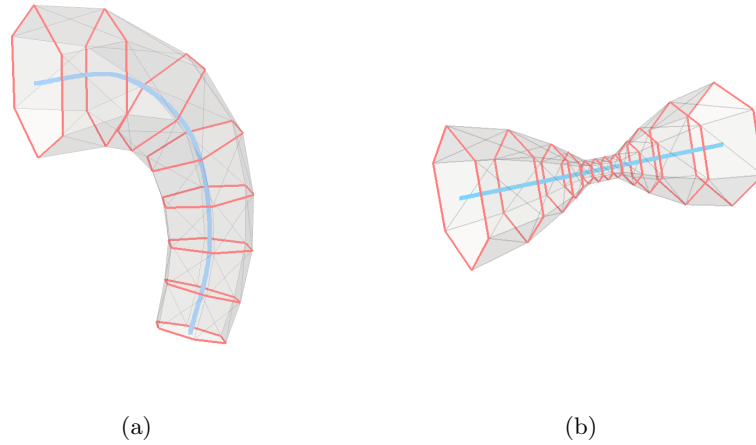
Figure 4: a) Hexagonal rings (red) placed along a curved centerline (blue) b) Hexagonal ring placement of the coarse mesh (red) for a varying vessel diameter.

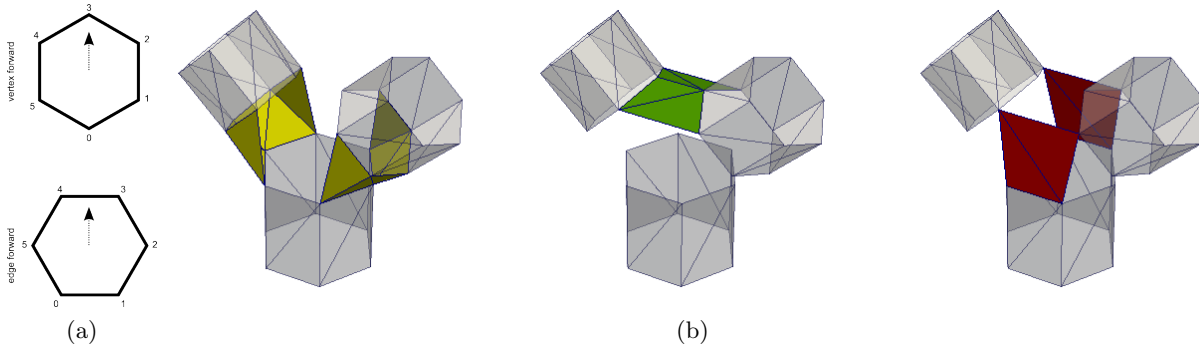(a)   (b)

Figure 5: a) Definition of the "vertex forward" (top) and "edge forward" (bottom) ring orientations. The arrow represents the normal vector of the bifurcation plane. The numbers indicate the local vertex numbering scheme used for describing the bifurcation (sub-)templates. b) Illustration of the different bifurcation sub-templates. From left to right: the left and right templates (yellow), the top template (green) and the bottom template (red). In this example all rings have the "edge forward" orientation.

regions is one of the major contributions of this work which is an adaptation of the earlier mentioned work of MacMurchy[8] (used for the modeling of plants) translated to vascular systems.

First, each ring in the bifurcation is classified by its orientation with respect to the bifurcation plane. The bifurcation plane is defined as the plane spanned by the three center positions of the hexagonal rings meeting at the bifurcation. The rings are classified as being either "vertex forward" or "edge forward" and a corresponding numbering scheme is used to label the vertices of each ring (see Figure 5a). Next, for each combination of ring classes in a bifurcation the optimal face connection scheme (called a template) is looked up in a pre-defined table and applied to connect the rings in the bifurcation. Using the defined vertex numbering scheme these templates can be described using a simple sequence of ids describing the triangles in the template. Different sub-templates are defined for the top, bottom, left and right side of a bifurcation (see Figure 5b). These sub-templates allow to easily extend beyond normal bifurcations to higher order junctions by combining multiple of them between the different ring pairs in the junction.

Figure 6 shows examples of a bifurcation and a trifurcation coarse mesh and the associated smooth subdivision surface.
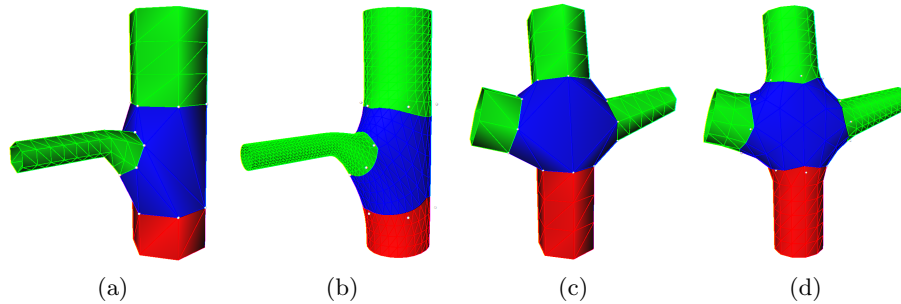
Figure 6: a) Example of a coarse mesh of a bifurcation with the trunk (red) and two branches (green) and the bifurcation template (blue). b) The smooth surface of the bifurcation in b) after two subdivision iterations. c) Example of a coarse trifurcation mesh. d) The trifurcation mesh of c) after two subdivision iterations.

2.2.4 Structural information

While constructing the coarse mesh, the structural information, e.g. which faces belong to a bifurcation or which vertices are part of the same hexagonal ring is stored. All of this structural information is also propagated from the coarse mesh to the subdivision surface. This information could for example be used to color code the surface based on its hierarchical position within the vascular tree (see Figure 6). It could also be used to easily identify and isolate particular branches in the tree. Another important aspect of having this structural information available is to quickly extract a new skeletal representations (centerlines with radii) from the current surface.
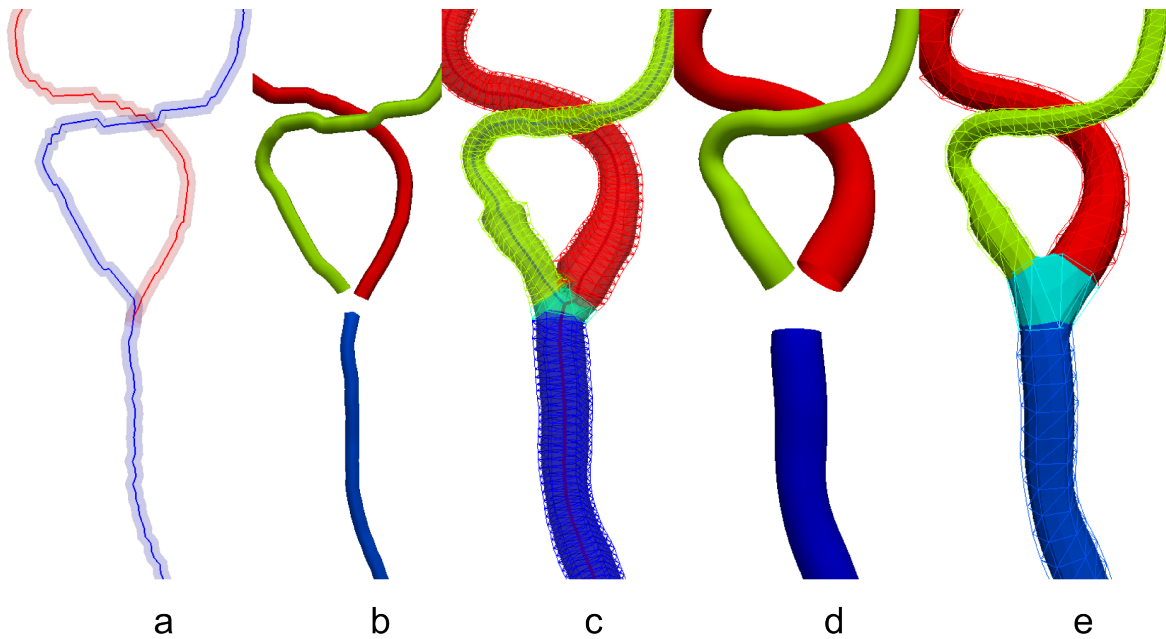

Figure 7: Overview of adaptive fitting process based on data of Challenge000 patient from cls2009.[1] From left to right: (a) initial centerlines. (b) branched centerlines with opened bifurcation region. (c) coarse mesh model after $N = 10$ fit iterations and new centerlines from surface. (d) branched updated centerlines and new bifurcation opening (e) final coarse mesh model and subdivision surface.

2.3 Adaptive Model Refinement

After a number of iterations the vertices of the hexagonal rings in the control mesh have moved with respect to their initial position. As a result the current size of the rings might no longer reflect the radius that was

used when the coarse mesh model was constructed. Since smaller ring distances are needed to capture the shape of smaller diameter vessels (and larger distances are allowed for larger vessel), the number of rings and their placement might need to be updated. Also, the size of the bifurcation region will require updating. Finally, considerable movement of the control vertices could result in self-intersection of the surface at certain locations. This is especially the case when the radii on the initial centerlines are much smaller than the true radii of the vessels to segment.

To overcome these issues we propose an adaptive model refinement. In the adaptive model refinement procedure, a new skeletal representation (centerlines with radii) is extracted from the current subdivision surface. By analyzing the surface points associated with the same hexagonal ring in the coarse mesh model new positions and radii can be computed for the different branches in the vessel tree. These centerlines and radii are then used to create a new coarse mesh model and corresponding subdivision surface. The fitting then continues using these updated structures. Figure 7 shows an example of the use of this adaptive model refinement.

3. EXPERIMENTS AND RESULTS

All the described methods were implemented in C++/Python within the MeVisLab (`http://www.mevislab.de`) framework. Segmentation experiments were performed on a PC with an Intel Xeon processor running four cores at 2.4 GHz.

3.1 CTA Images of the Carotid Artery Bifurcation

The segmentation method was applied to computed tomography angiography (CTA) image data of the Carotid Bifurcation Algorithm Evaluation Framework.[1] The complete dataset consists of 56 patient scans, which are split into 15 training and 41 testing sets. Exact imaging parameters are described by Hameeteman et al.[1] Furthermore, three positions inside the vessels (common, internal and external carotid artery) were provided by the evaluation framework. The segmentation method was evaluated using the 41 testing scans as described below.

First, centerlines were automatically detected. Centerlines where obtained using the provided proximal and distal target points in the data. A fast-marching wave propagation algorithm[10] with a vessel medialness[11] speed function was used to trace initial pathlines in the image data. Three centerlines needed manual correction. Next, a simple pre-processing step was applied to mask calcium regions along the vessels by thresholding the image. The threshold was calculated as the sum of the 95th percentile and the standard deviation of all voxel HU values extracted along the initial centerlines.

Next, the segmentation method was applied using the following parameters: the initial radii were set to 1 mm for all centerlines, a single subdivision step was used, the total number of fitting iterations was set to 40. The adaptive model refinement was performed after every 10 iterations. Scanlines were searched for edges from bright to dark (including the masked calcium regions), the scanline distance inside the model l^- was 1 mm and the distance outside the model l^+ was 2.5 mm. An α of 0.3 was used in each iteration to move the surface in small steps.

The segmentation results were submitted to the evaluation framework and achieved an average Dice similarity index of 89.2% [minimum 81.9%, maximum 94.8%], average mean surface distance of 0.59 mm [0.22 mm, 1.26 mm] and average Hausdorff surface distance of 11.26 mm [4.17 mm, 15.00 mm] on the 41 cases of the test set. The scores were ranked 6 out of 11. Considering the simple gradient magnitude image force factor used during the fitting this can be considered a good result. The segmentation of one dataset took less than 10 seconds, which is considerably faster than most of the alternative methods presented during the challenge.[1] More detailed results are available on `http://cls2009.bigr.nl/`. An example of a good and less good segmentation result are shown in Fig. 8.
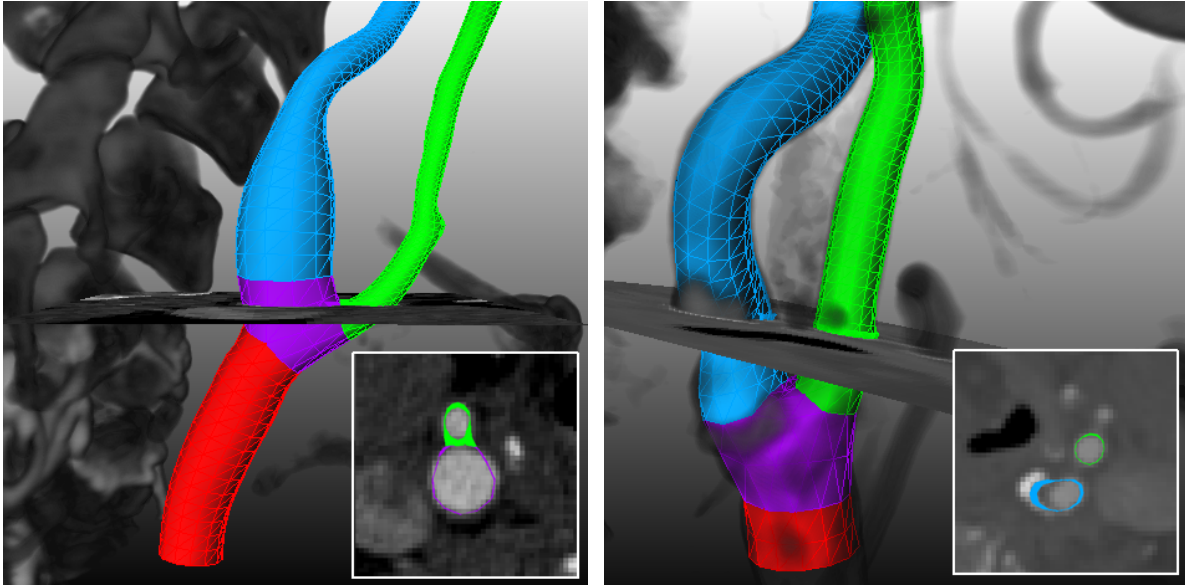
<div align="center">(a) (b)</div>

Figure 8: a) Good segmentation result Dice = 94.8% (Challenge014), b) Small error caused by calcified region Dice = 81.9% (Challenge020).
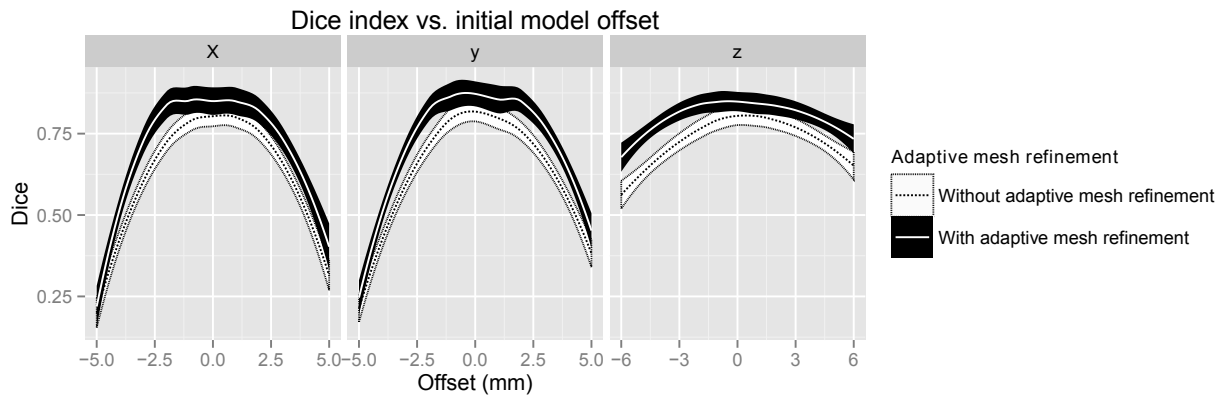

Figure 9: Average Dice index of segmentation results with ground truth data for the 15 training datasets as a function of the initial centerline displacement. Plots are shown for the method with and without the adaptive mesh refinement step.

3.1.1 Robustness analysis

To evaluate the robustness of the segmentation method to changes to the input centerlines and study the benefit of the adaptive model refinement step, the segmentation method was applied to the training data of the cls2009 framework with varying shifted (in x-, y-, and z-direction) versions of the original detected centerline. Also, each time the method was applied with and without the use of the adaptive model refinement step. Figure 9 shows the average Dice index for various displacements of the centerlines with and without refinement.

The method was robust to variations in centerline displacement up to 2 mm (mean diameter[12] of common carotid artery 6.52 ± 0.98mm). The results without the adaptive refinement step showed an overall lower Dice index and were less robust to changes in the initial centerline position.
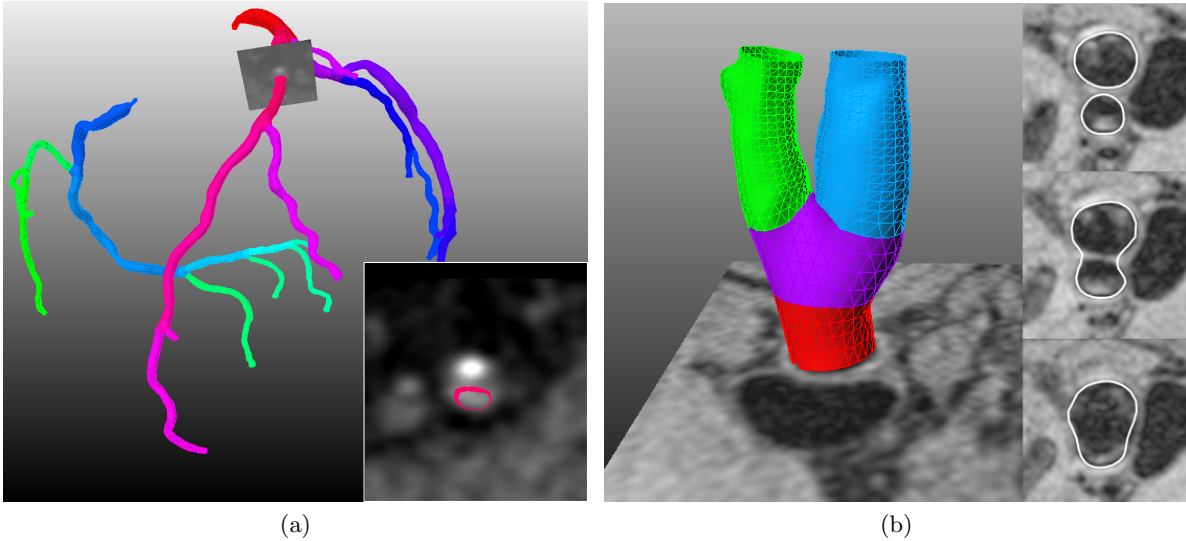
(a)
(b)

Figure 10: a) Example of fitting result on coronary arteries in CTA data (challenge patient 8 from[13]), b) a black blood MRI example.

3.2 Application to Complex Vascular Structures and MRI images.

To demonstrate the ability of the segmentation framework to adapt to different topological structures (not just single bifurcations), a coronary tree was segmented (Fig 10a) from a CTA image.[13] No adaptations to the mesh initialization algorithm was needed as the framework has intrinsic support for analyzing complex branching topologies. For the coronary tree dataset, 16 available centerlines were used to construct the initial coarse mesh consisting of 14 bifurcations. To perform the fitting the image force was calculated similar to the CTA carotid bifurcation dataset.

Also, a black blood MRI T1w vessel wall image of the carotid artery bifurcation was segmented (Fig. 10b) to show the application of the algorithm to a different modality than CTA. For this data, the image force was adapted such that the algorithm searches for an edge which is dark inside the model, and bright outside.

4. DISCUSSION AND CONCLUSION

A novel segmentation method for vascular structures based on fitting of subdivision surfaces was presented. Starting from a simple skeleton representation a coarse control mesh is generated. The generation of the control mesh geometry is facilitated by the use of dedicated bifurcation templates. A smooth surface is generated from the control mesh using a standard subdivision scheme. This surface is next iteratively fitted to image data using a simple gradient magnitude cost function. In addition, an adaptive refinement procedure is proposed to accommodate for changes in estimated initial vessel diameter and bifurcation geometry.

The results obtained using the CTA datasets of the carotid artery bifurcation show that the segmentation method is robust and provides competitive segmentation performance without using dataset specific optimizations. It is fast and no major changes were needed to apply the segmentation method to complex vascular structures or images from a different modality.

In future work more advanced image forces could be used to enhance the segmentation results. Also the influence of the various parameters used during the fitting like the number of iterations, the regularization parameter value and scanline properties could be investigated to improve on the current results. Finally, more application areas will be explored to further investigate the versatility of the proposed framework.

REFERENCES

[1] Hameeteman, K., Zuluaga, M., Freiman, M., and et al, "Evaluation framework for carotid bifurcation lumen segmentation and stenosis grading," *Medical Image Analysis* **15**, 477–488 (2011).

[2] Lesage, D., Angelini, E. D., Bloch, I., and Funka-Lea, G., "A review of 3D vessel lumen segmentation techniques: Models, features and extraction schemes," *Medical Image Analysis* **13**(6), 819 – 845 (2009).

[3] Manniesing, R., Schaap, M., Rozie, S., and et al, "Robust CTA lumen segmentation of the atherosclerotic carotid artery bifurcation in a large patient population," *Medical Image Analysis* **14**, 759–769 (2010).

[4] Li, K., Wu, X., Chen, D. Z., and Sonka, M., "Optimal surface segmentation in volumetric images–a graph-theoretic approach," *IEEE Trans Pattern Anal Mach Intell* **28**, 119–134 (2006).

[5] Orderud, F. and Rabben, S., "Real-time 3d segmentation of the left ventricle using deformable subdivision surfaces," in [*Computer Vision and Pattern Recognition, 2008. CVPR 2008. IEEE Conference on*], 1–8 (2008).

[6] Chandrashekara, R., Mohiaddin, R., Razavi, R., and Rueckert, D., "Nonrigid image registration with sub-division lattices: application to cardiac MR image analysis," in [*Medical Image Computing and Computer-Assisted Intervention - MICCAI 2007*], **4791**, 335–342 (2007).

[7] Loop, C., [*Smooth Subdivision Surfaces Based on Triangles*], Department of Mathematics, University of Utah (1987).

[8] MacMurchy, P., [*The use of subdivision surfaces in the modeling of plants*], Department of Computer Science, University of Calgary (2004).

[9] Antiga, L. and Steinman, D. A., "Robust and objective decomposition and mapping of bifurcating vessels," *IEEE Trans Med Imaging* **23**, 704–713 (2004).

[10] Janssen, J. P., Koning, G., de Koning, P. J. H., Tuinenburg, J. C., and Reiber, J. H. C., "A novel approach for the detection of pathlines in X-ray angiograms: the wavefront propagation algorithm," *Int J Cardiovasc Imaging* **18**, 317–324 (2002).

[11] Gulsun, M. A. and Tek, H., "Robust vessel tree modeling," in [*Medical Image Computing and Computer-Assisted Intervention - MICCAI 2008*], **5241**, 602–611 (2008).

[12] Krejza, J., Arkuszewski, M., Kasner, S. E., Weigele, J., Ustymowicz, A., Hurst, R. W., Cucchiara, B. L., and Messe, S. R., "Carotid artery diameter in men and women and the relation to body and neck size," *Stroke* **37**(4), 1103–1105 (2006).

[13] Kirisli, H. A., Schaap, M., Metz, and et al., "Standardized evaluation framework for evaluating coronary artery stenosis detection, stenosis quantification and lumen segmentation algorithms in computed tomography angiography," *Medical Image Analysis* **17**, 859–876 (2013).